Optical Properties of Ag and Cu

H. Ehrenreich and H. R. Philipp

General Electric Research Laboratory, Schenectady, New York

(Received July 6, 1962)

Experimental data for the optical constants of Ag and Cu extending to 25 eV are discussed in terms of three fundamental physical processes: (1) free-electron effects, (2) interband transitions, and (3)collective oscillations. Dispersion theory is used to obtain an accurate estimate of the average optical mass characterizing the free-electron behavior over the entire energy range below the onset of interband transitions. The values are $m_a = 1.03 \pm 0.06$ for Ag and 1.42 ± 0.05 for Cu. The interband transitions to 11 eV are identified tentatively using Segall's band calculations. Plasma resonances involving both the conduction band and d electrons are identified and described physically.

1. INTRODUCTION

IN a previous paper[1] the optical constants of silver were evaluated in the range between 1 and 10 eV by applying the Kramers-Kronig relations to reflectance data obtained near normal incidence. A re-examination of this data and its extension to higher energies appears appropriate at this time principally for two

(a)

(b)

FIG. 1. Spectral dependence of the reflectance of Ag and Cu. The data of Schulz are plotted below 3 eV (see reference 10).

reasons: A great deal has been learned recently concerning the structure of optical constants in the distinct regions where interband transitions and collective excitations predominate in groups 4 and 3–5 semiconductors.[2-5] This experience is almost directly applicable to metals. In addition, detailed band calculations for the noble metals are now available, particularly for copper.[6] Thus observed structure, which might be expected to result from interband transitions near symmetry points in the Brillouin zone, can be identified with the help of these calculations. It will be seen that this identification also leads to a better theoretical understanding of the behavior of the optical constants in the Drude region and, in particular, permits a more accurate estimate of the "optical" mass associated with the conduction band than has been possible heretofore.

This paper presents optical data for silver and copper in the energy range 1 to 25 eV. Results for the real and imaginary parts of the dielectric constant, ϵ_1 and ϵ_2, as well as the energy loss function $\operatorname{Im} \epsilon^{-1}(\omega)$ are presented in Sec. 2. The theoretical framework for interpreting these data is outlined in Sec. 3. The detailed discussion, in terms of specific interband transitions, collective excitations, and Drude free-electron behavior, as appropriate, appears in Sec. 4.

2. EXPERIMENTAL RESULTS

Reflectance data at 300°K for electrolytically polished bulk silver and copper surfaces are shown in Fig. 1.[7] The techniques employed in these measurements have been described elsewhere.[1] These samples are conceivably subject to atmospheric contamination and the data should be treated with some caution until further studies, admittedly very difficult, can be made on bulk
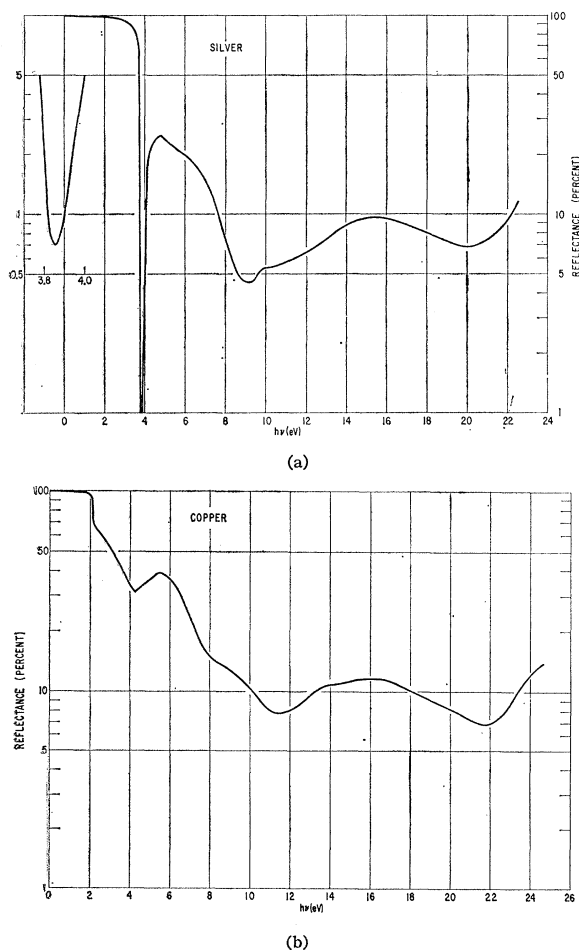
[2] H. Ehrenreich, H. R. Philipp, and J. C. Phillips, Phys. Rev. Letters 8, 59 (1962) and cited references.

[3] D. T. F. Marple and H. Ehrenreich, Phys. Rev. Letters 8, 87 (1962).

[4] H. Ehrenreich and H. R. Philipp, International Conference on Semiconductor Physics Exeter, July 1962 (to be published).

[5] D. Brust, J. C. Phillips, and F. Bassani (to be published).

[6] B. Segall, Phys. Rev. 125, 109 (1962). Preliminary results for silver and gold are given in General Electric Research Laboratory Report No. RL-2785G (unpublished). G. A. Burdick, Phys. Rev. (to be published).

[7] See also W. C. Walker, O. P. Rustgi, and G. L. Weissler, J. Opt. Soc. Am. 49, 471 (1959); G. B. Sabine, Phys. Rev. 55, 1064 (1939).

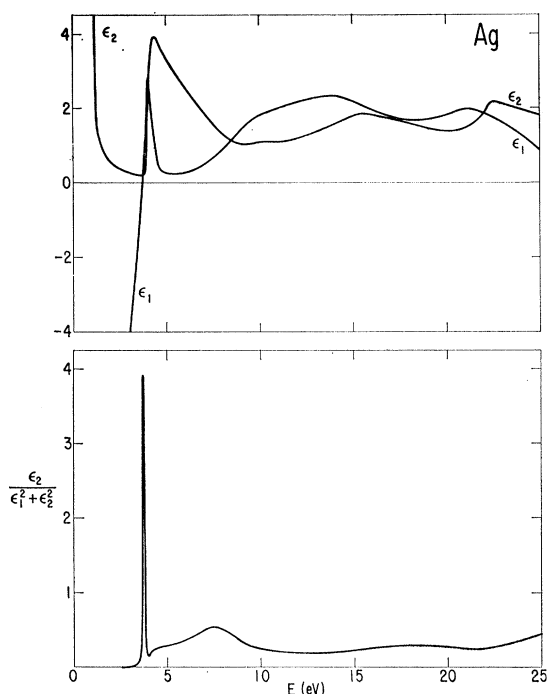[1] E. A. Taft and H. R. Philipp, Phys. Rev. 121, 1100 (1961).

FIG. 2. Spectral dependence of the real and imaginary parts of the dielectric constant and the loss function $\epsilon_2/(\epsilon_1{}^2+\epsilon_2{}^2)$ for Ag.

Here $\omega_{Pa}{}^2 = 4\pi n_c e^2/m_a$ is the square of the conduction band plasma frequency, n_c is the conduction electron density, $m_a{}^{-1} = (4\pi^3 n_c \hbar^2)^{-1} \int d^3k\ (1/3)\nabla_k{}^2 E_c(k)$ is the average inverse effective mass of the conduction electrons, the so-called "optical" mass defined by Cohen,[12] and τ_c is the possibly frequency-dependent relaxation time characterizing excited states in the conduction band. Further, $f_l(k)$ is the Fermi distribution function for state k in band l, $f_{l'l}{}^\mu$ is the oscillator strength as defined by Ehrenreich and Cohen,[13] $\tau_{ll'}$ is an interband relaxation time, and $\hbar\omega_{ll'} = E_l(k) - E_{l'}(k)$ where $E_l(k)$ is the energy of a Bloch electron k in band l. It is not necessary to distinguish explicitly here between the longitudinal and transverse dielectric constant since at least within the RPA the two are equal at long wavelengths.[14]

Equation (1) may be derived using the procedure of reference 13, but with the introduction of a collision term involving a band dependent relaxation time into the Louville equation. The specific form the collision term should assume is a matter of some controversy upon which we do not wish to enter here.[15] None of the forms commonly in use[16] lead to results which satisfy

surfaces prepared under conditions of ultrahigh vacuum. We consider the results adequate for the physical interpretation to to be discussed in this paper.

The dielectric constants are obtained from the above data by Kramers-Kronig analysis[8] and are shown in Figs. 2 and 3. The reflectance curve was extrapolated[9] beyond the last experimental point so as to make the calculated values for ϵ_1 and ϵ_2 agree with the careful measurements of Schulz[10] and Roberts[11] in the region near 1 eV. Also shown in Figs. 2 and 3 are values of the energy loss function $-\mathrm{Im}\epsilon^{-1} = \epsilon_2/(\epsilon_1{}^2+\epsilon_2{}^2)$ which is pertinent to the discussion below.

3. COMPLEX DIELECTRIC CONSTANT FOR A METAL

In the interpretation of some aspects of the preceding data, it is convenient to have at hand a tractable expression for the complex dielectric constant. Such an expression, applicable for a metal, and valid within the framework of the random phase approximation (RPA), is

$$\epsilon(\omega) = 1 - \omega_{Pa}{}^2/\omega(\omega + i/\tau_c)$$
$$- m^{-1}(e/\pi)^2 \int d^3k \sum_{ll'}{}' f_l(k)$$
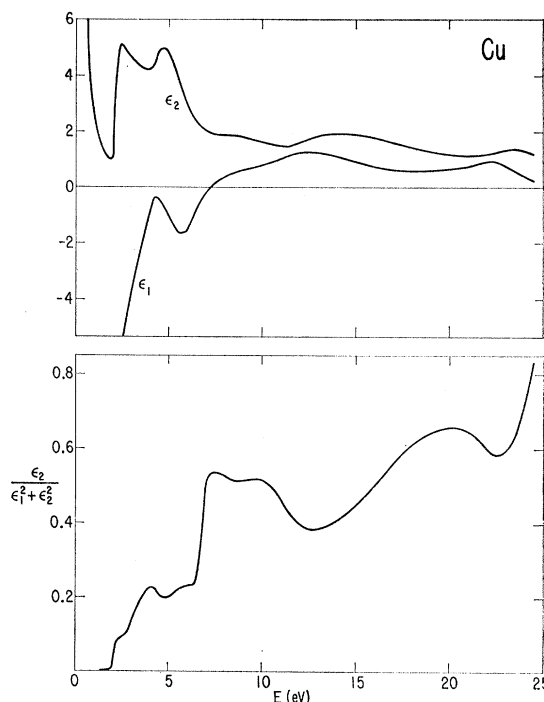$$\times f_{l'l}{}^\mu [(\omega + i/\tau_{ll'})^2 - \omega_{ll'}{}^2]^{-1}. \quad (1)$$

FIG. 3. Spectral dependence of the real and imaginary parts of the dielectric constant and the loss function $\epsilon_2/(\epsilon_1{}^2+\epsilon_2{}^2)$ for Cu.

[8] H. R. Philipp and E. A. Taft, Phys. Rev. 113, 1002 (1959).
[9] Beyond the last experimental point, the reflectance was linearly extrapolated in a plot of $\ln(R^{1/2})$ vs $\ln h\nu$ to 5% at 30 eV and to 0.216% at 100 eV for Ag and to 5% at 30 eV and to 0.0123% at 100 eV for Cu.
[10] L. G. Schulz, Suppl. Phil. Mag. 6, 102 (1957).
[11] S. Roberts, Phys. Rev. 118, 1509 (1960).
[12] M. H. Cohen, Phil. Mag. 3, 762 (1958).
[13] H. Ehrenreich and M. H. Cohen, Phys. Rev. 115, 786 (1959).
[14] S. L. Adler, Phys. Rev. 126, 413 (1962).
[15] This matter will be discussed by S. L. Adler and H. Ehrenreich (to be published).
[16] J. Lindhard, Kgl. Danske Videnskab. Selskab, Mat.-fys. Medd. 28, 8 (1954); R. Karplus and J. Schwinger, Phys. Rev. 73, 1020 (1948); M. S. Dresselhaus and G. Dresselhaus, ibid. 125, 499 (1962); H. Ehrenreich and H. R. Philipp, reference 4.
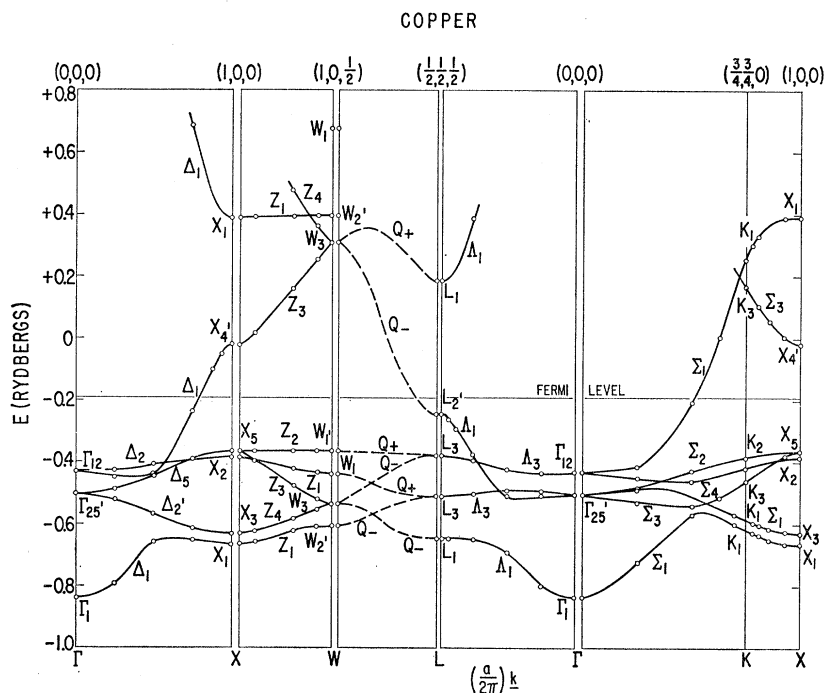
COPPER

FIG. 4. The calculated energy bands for Cu along the various symmetry axes in the Brillouin zone and on the zone surface according to Segall (see reference 6).

the continuity equation. We, therefore, choose to regard the relaxation time as a purely heuristic concept which permits a simple qualitative appreciation of broadening effects and which should be introduced so that the expression for the dielectric constant is as simple as possible, assumes the proper form in the limits of high and low frequencies, and reduces to the RPA value when $\tau \to \infty$. In the case of Eq. (1) we observe that the second, free-electron-like term has the standard Drude form[10] and leads to a finite conductivity for $\omega = 0$. On the other hand, the third, bound-electron-like, term leads to zero conductivity in this limit. In the tight-binding approximation the interband terms have a structure analogous to the Lorentz formula for an insulator.[17] The asymptotic frequency dependence is that required by the exact dielectric constant,[18] and as $\tau \to \infty$, Eq. (1) approaches the standard RPA result.[19]

It is useful to write Eq. (1) in the form

$$\epsilon(\omega) = \epsilon^{(f)}(\omega) + \delta\epsilon^{(b)}(\omega), \qquad (2)$$

which separates explicitly the free-electron contribution,

$$\epsilon^{(f)}(\omega) = 1 - \omega_{Pa}^2/\omega(\omega + i/\tau_c), \qquad (3)$$

from that due to the bound electrons.

[17] F. Seitz, *Modern Theory of Solids* (McGraw-Hill Book Company, Inc., New York, 1940), Chap. 17.

[18] P. Nozières and D. Pines, Phys. Rev. **113**, 1254 (1959).

[19] It may be noted in passing that Eq. (1) can be derived by introducing the collision term

$$\langle kl | \dot{\rho}_{\text{coll}} | k+q, l' \rangle$$
$$= -\tau_{ll'}{}^{-1}[\langle kl | \rho | k+q, l' \rangle - \alpha_{kl, k+q, l'} \langle kl | k+q, l' \rangle V(q,\omega)],$$
where
$$\alpha_{kl, k+q, l'} = [f_l(k) - f_{l'}(k+q)]/[E_l(k) - E_{l'}(k+q)] \quad \text{for} \quad l = l',$$
$$= 0 \quad \text{for} \quad l \neq l',$$
on the right-hand side of Eq. (28) of reference 13.

When a crystal, such as one of the noble metals, contains a set of partly filled conduction bands c, lower completely filled d-band d, as well as filled core states and empty excited bands, $\delta\epsilon^{(b)}$ may be written at 0°K as

$$\delta\epsilon^{(b)}(\omega) = -m^{-1}(e/\pi)^2 \left[\sum_{l \leq d} \int_{k > k_F} d^3k \, f_{cl}{}^\mu g_{cl} \right.$$

$$\left. + \sum_{l > c} \int_{k < k_F} d^3k \, f_{lc}{}^\mu g_{lc} + \sum_{l \leq d, l' > c} \int d^3k \, f_{l'l}{}^\mu g_{l'l} \right]. \qquad (4)$$

Here k_F denotes the wave number at the Fermi surface and $g_{l'l} = [(\omega + i/\tau_{ll'})^2 - \omega_{ll'}{}^2]^{-1}$. The form of Eq. (4) indicates that the interband terms associated with the conduction electrons are part of the bound-electron contribution to the dielectric constant. It should also be noted that $\delta\epsilon^{(b)}$ satisfies the Kramers-Kronig relations[20] since both $\epsilon(\omega)$ and $\epsilon^{(f)}(\omega)$ do. This fact may also be verified directly from Eq. (4).

4. DISCUSSION

The interpretation of the data is greatly facilitated if the different physical phenomena to be expected are clearly distinguished at the outset. These are (1) free-electron-like behavior at the lowest photon energies, (2) interband transitions at higher energies, and (3) collective oscillations, possibly in both regions. The qualitative behavior of the dielectric constant to be associated with each of these phenomena is already evident from previous work. The free-electron region

[20] L. D. Landau and E. M. Lifshitz, *Electrodynamics of Continuous Media* (Pergamon Press, New York, 1960), par. 62.

has been qualitatively described[10] by the Drude formula, Eq. (3), but often without considering the screening effects due to $\delta\epsilon^{(b)}$.[21] In the region where interband transitions dominate, the dielectric constants are expected to exhibit structure qualitatively similar to that in semiconductors.[4] Finally, the region where collective oscillations occur should be characterized by large values of the energy loss function $\mathrm{Im}\epsilon^{-1}(\omega)$ and small values of ϵ_1 and ϵ_2. It should be noted from the plots of $\mathrm{Im}\epsilon^{-1}(\omega)$ in Figs. 2 and 3 that the plasma and interband regions are not nearly as clearly disinguished as in the case of semiconductors[4] where the oscillator strengths for valence to conduction band transitions are almost exhausted as the plasma region is approached. It seems possible, nevertheless, to make a relatively unambiguous assignment of the data to any of the above physical phenomena for the noble metals. We now turn to a detailed discussion of each of them. For reasons which will become apparent, it will be convenient to discuss interband transitions before the free-electron or plasma effects.

A. Interband Transitions

For metals, the onset of interband absorption is associated with transitions from the Fermi surface to the next higher empty band or with transitions from a lower lying filled band to the Fermi surface. Interband absorption can be identified with the structure in the real and imagninary parts of the dielectric constant. The specific form of ϵ_1 and ϵ_2 depends on the location of the critical points[22] (i.e., singularities) in the joint density of states for the two bands participating in the transition.[3,5] Since critical points are most likely to occur at positions of high symmetry in the Brillouin zone, it seems reasonable to try to relate the structure in the dielectric constants or the absorption coefficient with the gaps as obtained from band theory at such locations.

The result of Segall's band calculations[6] for copper are shown in Fig. 4. The calculated low-energy gaps at or near symmetry points, which would be expected to correspond to photon energies where structure is observed, are most conveniently compared with the experimental absorption coefficient $\alpha = 4\pi k/\lambda$. The spectral dependence of this quantity is plotted for Ag and Cu in Fig. 5. The calculated gaps in question are indicated by arrows. These assignments appear to be reasonable in view of the fact that structure is indeed observed approximately where it is expected. However, in arriving at these identifications, a great deal of reliance must be placed on the accuracy of these calculations. Unfortunately, the sensitivity of the various gaps

to the crystal potential has not been tested as in the case of germanium.[23]

Segall has also obtained preliminary results for silver,[6] which are qualitatively very similar to those for copper, except possibly for the location of the d bands. He has pointed out that these results are probably somewhat less accurate than those for copper, since silver is a moderately heavy atom and the approximation entailed in the use of nonrelativistic atomic wave functions is less valid. The chief uncertainty appears to lie in the position of the d band relative to the Fermi surface. An empirical adjustment of this gap by a rigid translation of all the d levels might be expected to bring the gaps into better agreement with experiment. Segall estimates this to be a shift downward by about 2 eV for the first potential which he considered.

Because of the similarity of the band structure of copper and silver, the absorption spectrum of the two metals would also be expected to be qualitatively similar in the region where interband transitions predominate. That this is roughly the case can be seen by comparing the two curves in Fig. 5. Assignments given to structure
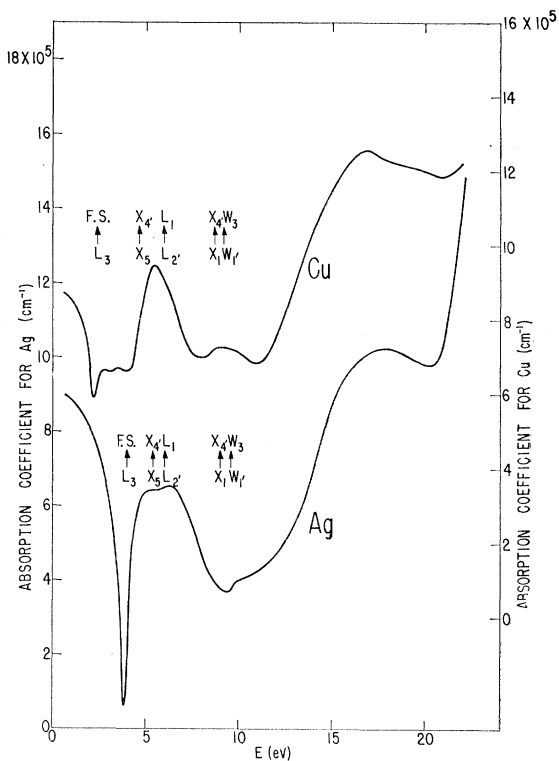

FIG. 5. Spectral dependence of the absorption coefficient ($\alpha = 4\pi k/\lambda$) of Ag and Cu. The arrows correspond to interband transitions at symmetry points obtained from Segall's calculations (reference 6). The Ag results contain an empirical adjustment, described in the text.

---

[21] Cohen's formalism (see reference 12) and Roberts' empirical formulas (see reference 11), however, contain provisions for such effects.

[22] L. van Hove, Phys. Rev. **89**, 1189 (1953); J. C. Phillips, *ibid.* **104**, 1263 (1956).

[23] F. Herman and S. Skillman, *Proceedings of the International Conference on Semiconductor Physics, Prague, 1960* (Czechoslovakian Academy of Sciences Publishing House, Prague, 1961), p. 20; J. C. Phillips, Phys. Rev. **125**, 1931 (1962).

in Cu can thus be related in an approximate way to the absorption curve of Ag. Segall's calculations for Ag yield a gap $L_{3'} \rightarrow$ Fermi surface of 2.2 eV which is to be compared to the experimental value of about 4 eV. If the gaps at this and other critical points are increased by 1.8 eV, the values indicated by the arrows in Fig. 5 corresponding to Ag are obtained. This procedure for adjusting the band structure of Ag is admittedly crude. It should, nevertheless, be sufficiently valid to permit assignment of the transitions if the identifications made for copper are also correct.

The reflectance of the noble metals in the energy region above 10 eV remains high and absorption coefficients rise considerably above 10^6 cm^{-1}. The identification of optical transitions in this range is more difficult since the number of possible transitions is greatly proliferated. In contrast to the case of semiconductors, the oscillator strengths appear to be rather widely distributed in energy. Some further appreciation of this fact can be obtained from consideration of the sum rule yielding n_{eff}, the effective number of electrons per atom contributing to the optical properties over a given frequency range, which has been previously used in connection with semiconductors.[24,4] In the case of the noble metals, and for $\epsilon^{(f)}$ and $\delta\epsilon^{(b)}$ as given by Eqs. (3) and (4), respectively, this sum rule takes the form

$$
\int_0^{\omega_0} \omega \epsilon_2(\omega) d\omega \equiv 2\pi^2 N n_{\text{eff}} e^2/m = \omega_{Pa}^2 \tan^{-1}\omega_0 \tau_c
$$

$$
+ (2m)^{-1}(e/\pi)^2 \left[\int_{k>k_F} d^3k \sum_{l \leq d} f_{cl}{}^{\mu} h_{cl}^-(\omega_0) \right.
$$

$$
+ \int_{k<k_F} d^3k \sum_{l>c} f_{lc}{}^{\mu} h_{lc}^-(\omega_0)
$$

$$
\left. + \int d^3k \sum_{l \leq d, l'>c} f_{l'l}{}^{\mu} h_{l'l}^-(\omega_0) \right]. \quad (5)
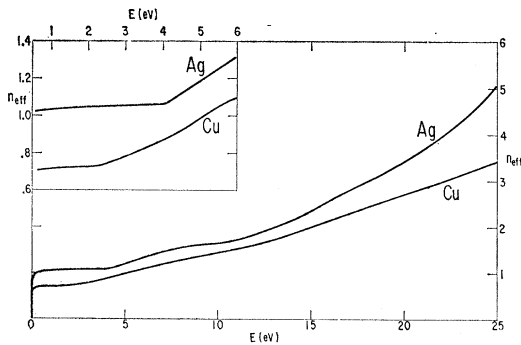$$

FIG. 6. Effective number of electrons per atom vs E obtained from numerical integration of experimental ϵ_2 using Eq. (5).

[24] H. R. Philipp and H. Ehrenreich, Phys. Rev. Letters **8**, 92 (1962).

Here N is the atom density of the crystal and $h_{l'l}^-(\omega_0)$ is the previously defined[4] quantity

$$
h_{l'l}^-(\omega_0) = \tan^{-1}(\omega_0 - \omega_{l'l})\tau_{l'l} + \tan^{-1}(\omega_0 + \omega_{l'l})\tau_{l'l}
$$
$$
- (2\omega_{l'l}\tau_{l'l})^{-1} \ln[(\omega_0 + \omega_{l'l})^2\tau_{l'l}^2 + 1]/
$$
$$
[(\omega_0 - \omega_{l'l})^2\tau_{l'l}^2 + 1], \quad (6)
$$

which is a step function in the limit $\tau_{l'l} \rightarrow \infty$. It results from the fact that the ϵ_2 describes real optical transitions which are energetically allowed only if ω_0 is larger than the threshold.

Equation (5) is an empirical modification of a rigorous result:

$$
\int_0^{\infty} \omega \epsilon_2(\omega) d\omega = 2\pi^2 N n e^2/m, \quad (7)
$$

where n is the total number of electrons per atom. If the core states can be neglected over the entire far vacuum ultraviolet range, then a numerical evaluation of n_{eff} using the experimental values of ϵ_2 in Eq. (5) should saturate at a value $n_{\text{eff}} = 11$ (1s plus 10d electrons) when the f sum is exhausted. This can be seen explicitly from an examination of the last member of Eq. (5) by observing that $h^-(\infty) = \pi$ and using the f-sum rule $\sum_{l'} f_{l'l}{}^{\mu} = 1 - (m/\hbar^2)\partial^2 E_l(k)/\partial k_\mu^2$. The rapidity with which n_{eff} approaches its saturation value as a function of energy, therefore, gives some information concerning the distribution of oscillator strengths. Figure 6 shows a plot of n_{eff} vs photon energy obtained for energies greater than 0.62 eV (2μ) from a numerical integration of the experimental ϵ_2. Unfortunately, neither the direct measurements of ϵ_2,[10,11] nor the extrapolation of the Kramers-Kronig analysis was capable of yielding sufficient information for a comparable treatment at lower energies. Hence $\epsilon_2^{(f)}$ as obtained from Eq. (3) was integrated analytically using the values of ω_{Pa} and τ_c discussed in the next section. The singularity of ϵ_2 at zero frequency causes n_{eff} to rise very rapidly to a value near unity in the present case. The deviation from unity is due to departures of the effective mass value from the free electron mass. Given sufficient data at low energies this deviation could be used to determine m_a. Figure 6 shows that n_{eff} essentially saturates at the free-electron value and is nearly constant until the threshold for interband transitions is reached. Equation (5) indicates that the initial increase at the threshold may result either from the excitation of d electrons to the Fermi surface or from the excitation of electrons at the Fermi surface to the lowest empty conduction band. The n_{eff} plot does not distinguish between these alternatives, although from the identifications that have been made by comparison with the band calculations we assign the increase to the former possibility.[25] The n_{eff} plot, how-

[25] It should be noted that Segall's calculations predict a Fermi surface in accord with experimental observations. Since the proximity of the d band will influence significantly the shape of the Fermi surface, this agreement provides strong support for this

ever, does indicate that the reflectance minima in Ag and Cu which occur at the same energy as the increase in n_{eff} are associated, at least in part, with the onset of interband transitions. The fact that n_{eff} increases very slowly and is for both Cu and Ag still far removed from the expected saturation value of 11 at 25 eV indicates that the oscillator strengths for transitions involving the d and/or s electrons are distributed over a rather wide energy range.

B. Free-Electron Effects

In the preceding subsection it was pointed out that interband transitions in Ag and Cu do not set in until a threshold energy $\hbar\omega_i = 3.9$ and 2.1 eV, respectively. It can, in fact, be seen from Figs. 2 and 3 that for both materials ϵ_2 falls off rapidly in the free-electron region, as expected from Eq. (3), and approaches a value close to zero (particularly in Ag) before the rise due to the onset of interband transitions ensues. This fact permits a relatively unambiguous separation of ϵ_2 into its "free" and "bound" contributions. In particular, since $\delta\epsilon_2^{(b)}$ describes real interband transitions, $\delta\epsilon_2^{(b)} = 0$ for $\omega < \omega_i$, aside from negligible broadening effects. To a sufficient approximation for the present purposes we may assume that $\epsilon_2^{(f)} = 0$ for $\omega > \omega_i$, so that the two contributions are supposed quantitatively separated. This fact may be used in conjunction with Eq. (2) and the Kramers-Kronig relations to calculate $\epsilon_1^{(f)}$ in the region $\omega < \omega_i$ from

$$\delta\epsilon_1^{(b)}(\omega) = (2/\pi)\int_{\omega_i}^{\infty} d\omega' \, \delta\epsilon_2^{(b)}(\omega')\omega'[\omega'^2 - \omega^2]^{-1},$$

$$\omega < \omega_i. \quad (8)$$

This numerical calculation is made simple by the fact that the denominator does not vanish over the entire range of integration. Since $\omega\tau_c \gg 1$ for most of the range of interest the only important undetermined constant is m_a. This can be obtained quite accurately by matching the calculated quantity $\epsilon_1^{(f)} + \delta\epsilon_1^{(b)}$ to the experimentally obtained $\epsilon_1(\omega)$. For these purposes it is sufficient to assume τ to have the value characteristic of the dc conductivity over the entire range. The results obtained in this manner are compared with the careful experimental results of Schulz[10] and Roberts[11] in Fig. 7. For Ag the two theoretical curves corresponding to $m_a = 0.96$ and 1.09 were obtained by matching, respectively, at 0.62 and 2.5 eV. The fact that the second value is somewhat larger than the first may be due to the fact that the excited states of the conduction band involved in the higher frequency transitions are characterized by a mass which is slightly larger than that directly at the

assignment. J. Rayne, [*The Fermi Surface*, edited by W. A. Harrison and M. B. Webb (John Wiley & Sons, Inc., New York, 1960), p. 226], has also reached a similar conclusion for Cu from studies of Cu-Zn alloys. On the other hand, M. Suffczynski, [Phys. Rev. **117**, 663 (1960)] assigned the onset of interband effects to transitions from the Fermi surface to a higher conduction band.
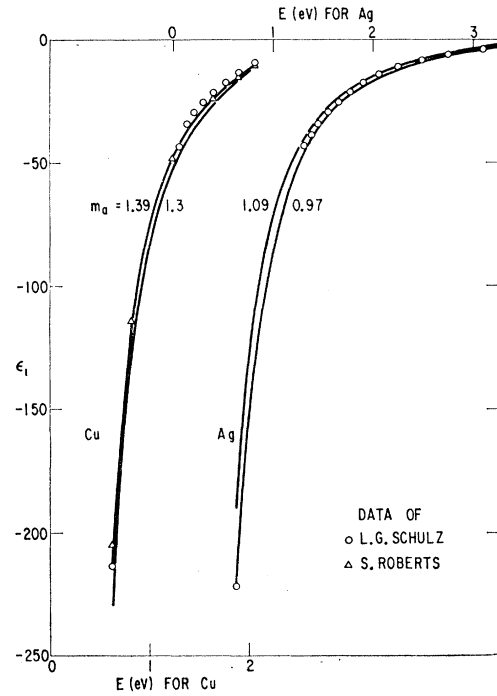

FIG. 7. Comparison of experimental and theoretical values of ϵ_1 for Ag and Cu in the "free-electron" region for several values of the optical mass m_a. The theoretical curve (solid line) is obtained using Eq. (2) with $\epsilon_1^{(f)}$ as given by Eq. (3) and $\delta\epsilon_1^{(b)}$ evaluated from the Kramers-Kronig relations. The points correspond to experimental data of Schulz (reference 10) and Roberts (reference 11).

Fermi surface. The spread between the two theoretical curves is probably characteristic of the error inherent in this method of estimating m_a.

In the case of Cu the curve corresponding to $m_a = 1.39$ was obtained by matching at 0.62 eV, and is seen to be in very good agreement with Robert's data. The calculated results corresponding to $m_a = 1.3$ use Segall's theoretical estimate for m_a and thus contain no adjustable parameters since τ_c can be neglected over the entire range. The best values for the average optical mass for the entire energy range, shown in Fig. 7, are $m_a = 1.03 \pm 0.06$ and $m_a = 1.42 \pm 0.05$ for Ag and Cu, respectively. These values are in good agreement with those due to Schulz[12] (0.97 ± 0.04 and 1.45 ± 0.06) and Roberts[11] (1.44 ± 0.01 for Cu). It should be noted that our value also lies within the uncertainty ± 0.1 of Segall's theoretical estimate of m_a.

The assumption that $\epsilon_2^{(f)}$ vanishes for $\omega > \omega_i$ produces an error of at most 3% in the value of m_a in Cu and somewhat less in Ag, as can be seen by subtracting the extrapolated contribution of $\epsilon_1^{(f)}$ in the region $\omega > \omega_i$ from the Kramers-Kronig integral.

The excellence of the agreement between theory and experiment in the preceding cases, of course, follows partly from dispersion theory and as such shows that the data given in Figs. 2 and 3 are consistent with the independent measurements of Schulz[10] and Roberts.[11]

However, the demonstrated applicability of Eq. (2) also leads us to the physical picture that the behavior in the Drude region may indeed be described by free electrons characterized by an average effective mass m_a, *provided* frequency-dependent screening effects arising from $\delta\epsilon^{(b)}(\omega)$ are also considered. The neglect of these effects is just the reason why the simple Drude theory agrees with experiments only at very low frequencies where $\epsilon_1^{(f)} \gg \delta\epsilon_1^{(b)}$.

It should be also reiterated that the preceding analysis is virtually independent of τ, and, in particular, of any model of introducing the interband relaxation times such as is exemplified in Eq. (4). It is, however, possible to estimate τ_c by using the values of m_a determined in the preceding analysis and requiring that the theoretical and experimental values of ϵ_2 agree over the range $\omega < \omega_i$. As might be expected, the relaxation time then exhibits a frequency dependence. One finds in the case of Ag that τ_c decreases from its dc value of 3.7×10^{-14} sec to 1.6×10^{-14} sec at 3 eV. Similarly in Cu, τ_c decreases from 3.5×10^{-14} at zero frequency to a value 1.6×10^{-14} sec at 2 eV. The actual character of the decomposition of $\epsilon^{(f)}$ and $\delta\epsilon^{(b)}$ will be discussed more fully in the next subsection in connection with plasma oscillations.

C. Plasma Oscillations

The general condition for the existence of plasma oscillations at a frequency Ω is $\epsilon(\Omega) = 0$.[26] The solution of this equation leads to a complex frequency $\Omega = \omega_P - i\Gamma$ whose real part corresponds to the plasma frequency ω_P
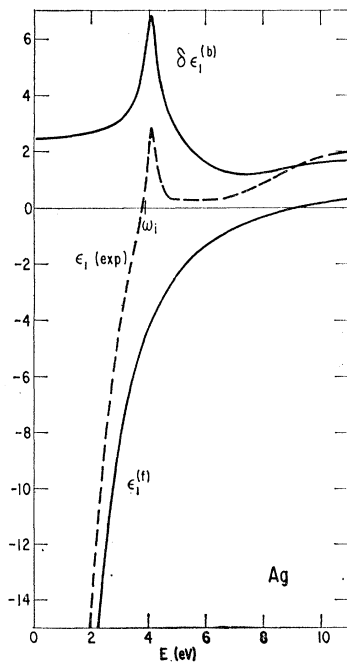

FIG. 8. Decomposition of the experimental values of ϵ_1 for Ag into free and bound contributions $\epsilon_1^{(f)}$ and $\delta\epsilon_1^{(b)}$. The threshold energy for interband transitions is indicated by ω_i.

and whose imaginary part Γ describes the damping of the plasma oscillation. When the damping is small, i.e., when $\epsilon_2(\omega_P) \ll 1$, the condition for plasma resonance may be written approximately as $\epsilon_1(\omega_P) = 0$. This equation, in fact, leads to the standard plasma dispersion relation in the free-electron case.[27] In general, however, it is not necessary that ϵ_1 vanish near the resonance frequency. In practice, a plasma resonance can be identified by the characteristic maximum in $\mathrm{Im}\,\epsilon^{-1}$ and distinguished from an interband transition by the fact that both ϵ_1 and ϵ_2 are small in the vicinity of the maximum in the loss function.

In connection with the identification of plasma resonances in Ag and Cu, it is useful to refer to Figs. 8 and 9 which show the decomposition of ϵ_1 into free and bound contributions which were obtained in the preceding section, and also to Figs. 2 and 3 which show the behavior of ϵ_2. In the absence of interband transitions, ϵ_1 would be given by $\epsilon_1^{(f)}$ and ϵ_2 would vanish substantially for frequencies greater than ω_i. The plasma resonance would occur where $\epsilon_1 = 0$, i.e., $\omega = \omega_{Pa}$, the value calculated for the density of free electrons having mass m_a given above. Figures 8 and 9 indicate that $\hbar\omega_{Pa} = 9.2$ and 9.3 eV for Ag and Cu, respectively. When interband transitions contribute, this simple picture may no longer be valid, since the contribution of $\delta\epsilon^{(b)}$ may be such as to cause ϵ_1 to be zero or nearly zero in a region where ϵ_2 is also small. This is precisely the situation in silver where the increase in ϵ_1 due to the incipient d band to Fermi surface transition causes ϵ_1 to vanish at an energy below ω_i, the threshold for this transition. Thus, as is seen from Figs. 3 and 8, where ω_i is explicitly indicated, ϵ_2 is still very small where ϵ_1 vanishes. Figure 3 also shows a very sharp peak in the energy loss function $\mathrm{Im}\,\epsilon^{-1}(\omega)$ at this energy, thus indicating that the conditions for plasma resonance are satisfied. This is not a free-electron resonance but rather a hybrid resonance resulting from the cooperative behavior of both the d and conduction electrons. Alternatively, this resonance may be described as due to the conduction electrons screened by a frequency-dependent dielectric constant. This can be seen directly from the condition for plasma resonance obtained from Eqs. (3) and (4) when τ_c is neglected:

$$\epsilon(\omega) = [1 + \delta\epsilon^{(b)}(\omega)](1 - \omega_P^{*2}/\omega^2) = 0. \qquad (9)$$

Here $\omega_P^{*2} = 4\pi n e^2/m_a(1 + \delta\epsilon^{(b)})$ is just the square of the screened plasma frequency. Since $\omega_P^* < \omega_i$, $\delta\epsilon^{(b)}(\omega) = \delta\epsilon_1^{(b)}(\omega)$ is real. The energy loss function peaks again at 7.5 eV near the free-electron plasma frequency. In this region neither ϵ_1 nor ϵ_2 vanishes but both are small. This fairly broad resonance is associated essentially with the conduction electrons, but depressed in energy from the free-electron value by strong interband transitions at higher energies. It is observed because the interband

[26] H. Fröhlich and H. Pelzer, Proc. Phys. Soc. (London) A68, 525 (1955).

[27] For example, R. A. Ferrell, Phys. Rev. 107, 450 (1957).

transitions are again relatively weak in this region and the behavior of ϵ_1 is qualitatively free electron like.

In copper, on the other hand, only the free-electron-like resonance is observed: Near 7.5 eV both ϵ_1 and ϵ_2 are small and the loss function has a maximum. The low-energy resonance is not present. In spite of the fact that $\delta\epsilon^{(b)}$ due to the d band to Fermi surface transition is larger in copper than in silver, $\epsilon_1^{(f)}$ is not increased sufficiently by $\delta\epsilon^{(b)}$ to satisfy the plasma condition since the interband transition in question occurs at a lower energy where $\epsilon_1^{(f)}$ is considerably more negative. The existence of the lowered plasma energy in silver is, therefore, seen to be a somewhat accidental consequence of the particular energetic position of the d band to Fermi surface transition and its strength. In this connection it may be noted that Wilson[28] has already discussed the influence of interband transitions on the free-electron plasma frequency. He observed, in particular, that an interband transition above the free-electron plasma frequency tends to depress its value. The situation in Ag concerning the lowered plasma loss is consistent with this picture.

The foregoing discussion clarifies the reason for the existence of the sharp reflectance minimum in Ag. The reflectance drops initially due to the presence of the very weakly damped plasma resonance and then rises abruptly because of the onset of interband transitions about 0.1 eV above the plasma energy.

It is also of interest to compare the results of characteristic energy loss experiments with the present data. For Ag, Robins[29] finds losses at 4.1, 7.3, and 17.2 eV, whereas for Cu, Powell[30] observes losses at 4.4, 7.2, and 19.9 eV. These should be compared with the maxima in $\epsilon_2/(\epsilon_1^2+\epsilon_2^2)$ plotted in Figs. 2 and 3. Corresponding
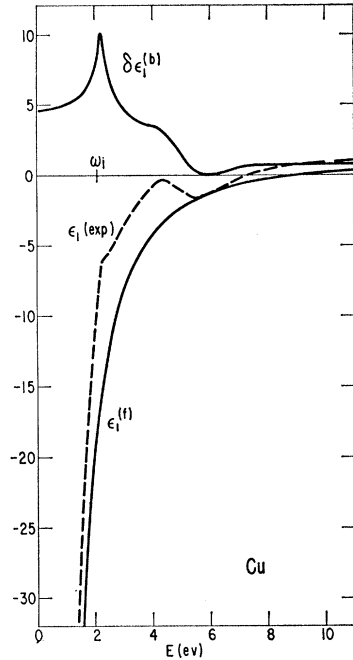

FIG. 9. Decomposition of the experimental values of ϵ_1 for Cu into free and bound contributions $\epsilon_1^{(f)}$ and $\delta\epsilon_1^{(b)}$. The threshold energy for interband transitions is indicated by ω_i.

structure is observed at 3.8, 7.5, and 18 eV for Ag, and at 4.1, 7.5, and 20 eV for Cu. Additional fine structure, not observed in the electron transmission experiments, is also present in the optical data.

ACKNOWLEDGMENTS

[28] C. B. Wilson, Proc. Phys. Soc. (London) **76**, 481 (1960).
[29] J. L. Robins, Proc. Phys. Soc. (London) **78**, 1177 (1961).
[30] C. J. Powell, Proc. Phys. Soc. (London) **76**, 593 (1960).